

Characterizing the role of Canoe as a cell junction-cytoskeletal linker protein during
Drosophila morphogenesis

Halle Ronk
Mark Peifer Laboratory
Biology Department, UNC-Chapel Hill
20 April 2018

ABSTRACT

Adherens junctions (AJs) connect epithelial cells to one another and connect the plasma membrane to the actomyosin cytoskeleton; this organization translates contractility to neighboring cells and preserves tissue integrity during morphogenesis. The exact interactions among adhesion molecules located at AJs remain unclear. It is currently thought that cadherins mediate cell-cell adhesion, while proteins bound to their cytoplasmic tails, known broadly as catenins, interact with junction-linker proteins. These linker proteins, in turn, interact with the actomyosin cytoskeleton. We examined whether Canoe acts as a junction-linker protein by testing its role in maintaining epithelial integrity, which is an indicator of junctional integrity. We used immunofluorescence and confocal microscopy to examine *Drosophila melanogaster* embryos during dorsal closure. In wild-type embryos, Canoe is enriched at the leading-edge epidermis and at multicellular junctions along the lateral epidermis. This enrichment pattern aligns closely with the location of actin filaments and myosin II heavy chain. We used RNA interference in conjunction with the UAS-Gal4 system to reduce *canoe* function. Loss of *canoe* caused cells along the lateral epidermis to become highly variable in shape, suggesting that translation of contractility to AJs occurred unevenly among the cell population. Furthermore, the number and regularity of puncta of Enabled, an actin assembly and elongation factor usually enriched at AJs, decreased along the leading edge. These results support the hypothesis that Canoe acts as a linker protein, playing an essential role in regulating epithelial sheet integrity and contractility. Understanding these complex interactions can provide insight into the mechanisms of wound healing and neural tube closure in humans and guide the creation of embryonic defect prevention therapies.

INTRODUCTION

Cell adhesion – the process by which cells attach to a surface, substrate, or other cells – is a fundamental cellular property, underlying processes from bacterial colonization to cancer metastasis. We explore cell adhesion in epithelia, the most common tissue architecture in animals. Epithelial cells form structures as diverse as the skin, kidney, and bronchioles. Given its wide distribution in the body, epithelia perform a variety of functions, from protection to excretion to gas exchange.

Cells in an epithelium exhibit a simple morphology with a distinct apical “top” and basal “bottom” polarity. The apical surface is usually exposed to fluid or the air, while the basal surface is attached to a basement membrane. Cadherin-based cell-cell adherens junctions (AJs) reside at the interface between the apical and basal domains. Cadherins mediate cell-cell adhesion, while proteins bound to their cytoplasmic tails, known broadly as catenins, interact with the actomyosin cytoskeleton (Meng and Takeichi, 2009). Blocking cadherin-catenin function disrupts cell adhesion in cultured epithelial cells and developing embryos (Cox et al., 1996; Gumbiner et al., 1988; Johnson et al., 1986). Defining roles for AJs in maintaining epithelial cell adhesion raised a new question: what adhesion molecules are essential for maintaining epithelial sheet integrity during embryo development, and how do these molecules interact with one another?

Fruit fly (*Drosophila melanogaster*) dorsal closure provides an excellent model for epithelial integrity. Dorsal closure is driven by dynamic remodeling of the actomyosin cytoskeleton at AJs along the leading-edge epidermis. During early closure, the leading-edge cells become organized into well-defined rows in which actin and myosin II cables assemble to form supracellular “purse strings” (Young et al., 1993; Kierhart et al., 2000). Tension in these

actin and myosin cables produces forces that maintain a uniform epithelial advance as the adjacent amnioserosal cells apically constrict (Kierhart et al., 2000). Eventually the amnioserosa is enclosed within the epidermis, and its molecular components are recycled by apoptosis (Kierhart et al., 2000). When the lateral epidermis fails to seal over the amnioserosa, a “dorsal open” phenotype is produced (Takahashi et al., 1998). In these “dorsal open” mutants, the underlying mesoderm remains exposed, and the embryos die (Takahashi et al., 1998).

Because AJs play a vital role during embryogenesis, they remain an active field of study. In the conventional model, cadherins link directly to actin via α - and β -catenin (Pokutta et al., 2002; Rimm et al., 1995; Drees et al., 2005). Later work revealed that this linkage is mediated by a far more sophisticated set of interactions (Yamada et al., 2005). This discovery prompted the search for so-called junction-linker proteins that regulate epithelial cell adhesion and AJ/cytoskeletal linkage.

One candidate junction-linker protein is Canoe. Canoe is homologous to the mammalian PDZ protein Afadin (AF-6), which plays critical roles in regulating intracellular signaling and organizing cell junctions throughout development (Brody 1998). Canoe’s own multidomain structure allows it to interact directly with the cytoskeleton via its F-actin-binding domain and to bind AJ proteins, including E-cadherin and α -catenin, via its PDZ and proline-rich domains (Mandai et al., 2013).

Early studies of *Drosophila* Canoe suggest that it is not essential for maintaining cell-cell adhesion, but it is required for many processes driven by AJ/cytoskeletal linkage (Sawyer et al., 2009). Studies examining zygotic *canoe* mutants in flies have demonstrated that loss of *canoe* leads to abnormal cell shape changes, asymmetric divisions, and aberrant cell fate choice in the nervous system and mesoderm (Jürgens et al., 1984; Takahashi et al., 1998; Boettner et al., 2003;

Carmena et al., 2006; Speicher et al., 2008). In *Drosophila*, loss of *canoe* hampers actomyosin-driven processes, such as apical constriction during gastrulation, convergent elongation during germband extension, and epithelial sheet migration during dorsal closure (Boettner et al., 2003; Boettner and Van Aelst, 2007; Sawyer et al., 2009; Choi et al., 2011; Sawyer et al., 2011).

These observations suggest that Canoe plays a pivotal role in regulating AJ/cytoskeletal linkage during *Drosophila* embryogenesis; however, the exact mechanisms and interactions by which Canoe exerts its effects remain unclear. In this study, we examine whether Canoe acts as a junction-linker protein by testing its role in maintaining epithelial integrity, which is an indicator of junctional integrity. We use immunofluorescence and confocal microscopy to examine *Drosophila melanogaster* embryos during dorsal closure. We use RNA interference in conjunction with the UAS-Gal4 system to reduce *canoe* function. We investigate the interactions between Canoe and AJ-associated molecules to examine how Canoe acts as a linker protein. Understanding these complex interactions can provide insight into the mechanisms of wound healing and neural tube development in humans – two processes that closely resemble *Drosophila* dorsal closure. This information, in turn, can assist in the creation of embryonic defect prevention therapies.

METHODS

Fly stocks

Fly stocks are listed in Table 1. Mutations are described at <http://flybase.org>. Wild-type included *yellow-white*, *Histone-GFP*, *E-cadherin-GFP*, and *Zipper-GFP (II)*. Various-strength *canoe* knockdown mutants were generated by crossing female virgins from the UAS-Gal4 *canoe* shRNA lines to males from the maternal driver lines as described in Blair (2003). The UAS-Gal4 *canoe* shRNA lines were the weaker UAS.*cno* RNAi Valium 20 (III) line and the stronger UAS.*cno* RNAi Valium 22 (II) line. The two maternal driver lines were the weaker triple maternal driver, abbreviated MTD-Gal4 (I,II,III), and the stronger double maternal driver, denoted Mat-Gal4 (II,III). The progeny from these crosses are described in Table 1. Previous work in the Peifer lab involved the *cnoR2*, *cnoMZ*, and *VP16:nos-Gal4* lines (Manning and Sewell, unpublished). All experiments were performed at 25 °C unless noted otherwise. Fly stocks were obtained from the Bloomington *Drosophila* Stock Center.

Preparation of cuticles and hatch rates

Cuticle preparations were made as described in Wieschaus and Nüsslein-Volhard (1986). Mutant *canoe* embryos from a single cross were collected and arranged into columns on an apple juice agar plate. The embryos were incubated for 48 hours at 25 °C, after which the number of hatched and unhatched embryos were recorded. Unhatched embryos were dechorionated in 50 % bleach, washed in 0.1 % Triton X-100(Sigma Aldrich cat. T9284), and incubated on microscope slide in Hoyer's:lactic acid overnight at 65 °C. The unhatched embryos were visualized via light microscopy to confirm the hatch rate predictions and classify the severity of embryonic defects.

Immunofluorescence

The staining protocol was adapted from Müller and Wieschaus (1996). Embryos were bleach dechorionated and fixed for 20 minutes in 1:1 4 % formaldehyde(Electron Microscopy Sciences cat. 15686)/PBS/0.5M EGTA:heptane(Sigma Aldrich cat. 34873). Embryos for hand-peeling were fixed for 30 minutes in 1:1 18 % formaldehyde/PBS/0.5M EGTA:heptane. Embryos that were not hand-peeled were devitellinized with methanol(Macron Fine Chemicals cat. UN1230). All embryos were blocked and stained in PBS/1 % normal goat serum(Fisher Scientific cat. NC9270494)/0.1 % Triton X-100(Sigma Aldrich cat. T9284). Primary and secondary antibodies were diluted in PBS containing 1 % normal goat serum and 0.1 % Triton X-100 and incubated overnight at 4 °C. Antibodies and probes are listed in Table 1.

Image Acquisition and Manipulation

Fixed embryos were mounted in Aqua-Poly/Mount (Polysciences) and imaged on a confocal laser-scanning microscope (LSM 710, 40x/NA 1.3 Plan-Apochromat oil objective, Carl Zeiss). ZEN 2009 software (Carl Zeiss) was used to process images and render z-stacks in 3-D. Maximum intensity projections (MIPs) were generated by acquiring z-stacks through the embryo with a 0.13 μm step size and digital zoom of 0.6 or 2.0. Photoshop CS6 (Adobe) and ImageJ (NIH) were used to adjust input levels so that the signal spanned the entire output grayscale and to adjust brightness and contrast.

RESULTS

Organization of epithelial AJs during wild-type dorsal closure

Our goal was to define the mechanisms mediating AJ/cytoskeletal linkage with a focus on how Canoe interacts with AJ-associated molecules. Our investigation was accomplished by using dorsal closure as a model system. We began our study with a question: where is Canoe typically enriched in wild-type embryos in relation to known adhesion molecules?

At the onset of dorsal closure, Canoe is positioned apically in lateral epidermal (LE) cells. While Canoe is visible around the entire apical perimeter of these cells, Canoe's distribution is not completely uniform. Canoe appears enriched at AJs along the leading edge, where LE meets the amnioserosa (AS) (Fig. 1A', yellow arrows). Canoe also appears enriched at tri- and multicellular junctions in LE cells that are not part of the leading edge (Fig. 1A', blue and red arrows). Since multicellular junctions are known to be regions of elevated contractility in other contexts, this enrichment pattern suggests that Canoe is recruited to areas of high tension to help modulate cell adhesion (Choi et al., 2016).

Early in dorsal closure, Armadillo [the β -catenin homolog] appears enriched along the leading-edge epidermis. Unlike Canoe, which is enriched at LE-LE bicellular junctions along the leading edge, Armadillo appears enriched *in between* these junctions during early dorsal closure (Fig. 1B', yellow arrows). As dorsal closure progresses, Armadillo appears to relocalize from the LE-AS cell borders to LE-LE cell borders (Fig. 1C', yellow arrows). This pattern is also consistent at the canthi, where the two lateral epidermal sheets meet the dorsal midline (Gorfinkiel and Arias, 2007). The bright spots that occur where the LE-LE cell borders meet the leading edge correspond to actin-nucleating centers (Fig. 1C', red arrows; Gorfinkiel and Arias, 2007).

To visualize actin, we stained hand-peeled embryos with phalloidin, which binds to F-actin. The enrichment pattern of actin closely mirrors that of Canoe. Actin is visible at the apical perimeters of LE cell borders (Fig. 2A', red arrows). Actin also appears significantly enriched at LE-LE bicellular junctions along the leading edge and slightly enriched at multicellular borders in the LE (Fig. 2A', yellow and blue arrows). These results raised the question, to what extent do Canoe and actin localize together?

Other studies in the Peifer lab are using super-resolution microscopy to investigate the localization of Canoe and actin at AJs along the leading edge. While Canoe is visible at the LE-LE bicellular junctions, actin fibers end just prior to these junctions (Manning, unpublished). These results suggest that Canoe is positioned at the AJ and may interact with the ends of actin fibers (Manning, unpublished).

These confocal and super-resolution studies of Canoe and actin support the hypothesis that multicellular junctions in the LE and bicellular junctions along the leading edge represent areas of increased tension and contractility. If Canoe and actin do indeed localize close to one another, Canoe could interact with actin filaments to regulate AJ/cytoskeletal linkage. This modulation would be especially important for maintaining epithelial integrity in the LE as these cells undergo shape changes and collective migration.

During dorsal closure, F-actin colocalizes with myosin II at the leading-edge epidermis to form the supracellular purse strings that cinch to seal the dorsal hole (Franke et al., 2005). To visualize myosin, we examined *Zipper-GFP (II)* embryos, a line that carries myosin II heavy chain tagged with green fluorescent protein. Similar to Armadillo, the myosin II fibers are predominantly located *between* LE-LE bicellular junctions along the leading edge (Fig. 2B', yellow arrows). As dorsal closure progresses, the myosin II enrichment pattern increases in

intensity. This phenomenon likely occurs because the myosin II fibers are pulled closer together as the dorsal hole shrinks rather than reflecting a greater number of myosin II fibers being recruited to the leading edge.

Interestingly, myosin II fibers form an alternating sequence with puncta of Enabled across the leading edge (Fig. 2B''', green and red arrows). Enabled is an actin-associated molecule that localizes to the plus ends of actin filaments to regulate the assembly of contractile cables and cell protrusions (Scott et al., 2006). Whereas myosin II fibers are located primarily *between* LE-LE bicellular junctions along the leading edge, puncta of Enabled are located *at* the junctions (Fig. 2C', blue arrows). This difference in enrichment produces an alternating myosin II - Enabled pattern across the leading edge.

Enabled also surrounds the borders of LE cells that are not part of the leading edge. Enabled is particularly noticeable among the groove cells that mark the boundary of each ventral segment (Fig. 2C', yellow arrows). Actin also appears enriched the segmental groove cells (Fig. 2D', yellow arrows). This enrichment becomes more noticeable at groove cells located farther away from the leading edge (Fig. 2D', red arrows). Thus, the enrichment pattern of Enabled aligns more closely with F-actin and Canoe than it does with myosin II. These results are consistent with the hypothesis that Enabled binds to the tips of F-actin cables and interacts with Canoe at AJs.

Strength of *canoe* knockdown affects the severity of embryonic defects

Examining adhesion molecules in wild-type embryos provided a baseline for typical enrichment levels. We continued our investigation by asking what changes in these enrichment patterns would occur when zygotic *canoe* levels are significantly reduced. We utilized RNA

interference in conjunction with the UAS-Gal4 system to generate *canoe* knockdown lines (Fig. 3A). Expression in the female germline knocks down maternal mRNA, and maternally-expressed Gal4 persists zygotically, driving zygotic shRNA expression, often leading to knockdown mimicking maternal/zygotic mutants (Staller et al., 2013).

The first attempts at knocking-down *canoe* involved the creation of maternal-zygotic *canoe* mutant lines. While these lines successfully knocked-down *canoe*, fertility issues and low embryo yields posed significant obstacles. The second attempts at knocking-down *canoe* involved the examination of zygotic *canoe* mutant lines. Finally, different degrees of *canoe* knockdown were obtained by crossing males from three different maternal driver lines to UAS.*cno* RNAi Valium 20 (III) virgin females and examining their progeny (Manning and Sewell, unpublished). The maternal drivers included the weak *VP16:nos-Gal4* driver, the intermediate MTD-Gal4 driver, and the strong Mat-Gal4 driver. These results indicated that this method of knocking-down *canoe* could successfully produce *canoe* mutant phenotypes of a range of severities.

In this study, we examined two new ways of reducing Canoe levels in embryos: (1) crossing the intermediate MTD-Gal4 driver to UAS.*cno* RNAi Valium 22 (II) females, and (2) crossing the strong Mat-Gal4 driver to UAS.*cno* RNAi Valium 22 (II) females. Based on previous work with the Valium 22 RNAi line, we expected that this RNAi line would produce a stronger knockdown compared to the Valium 20 RNAi line (Bonello et al., 2018).

RNAi severely reduced Canoe levels. The Valium 22 RNAi line reduced Canoe below levels detectable by immunoblotting, and only small amount of Canoe was visible from the Valium 20 RNAi line (Fig. 3B; Bonello et al., 2018). To determine how zygotic loss of *canoe* affects embryo viability, we analyzed the hatch rate of *canoe* knockdown lines. The unhatched

embryos were later visualized via light microscopy because cuticle phenotypes represent a read-out of the severity of epidermal defects (Fig. 3C-H).

Interestingly, our new MTD-Gal4; UAS.*cno* RNAi Valium 22 (II) mutants displayed a wide range of phenotypes, from embryos with no observable defects to those with severe morphogenetic defects (Fig. 3I). These results were unexpected because our new *cnoe* mutants displayed mild defects more frequently than the milder MTD-Gal4; UAS.*cno* RNAi Valium 20 (III) mutants. Furthermore, our new *cnoe* mutants also displayed cuticle fragments – the most severe phenotype – more frequently than the more severe Mat-Gal4; UAS.*cno* RNAi Valium 20 (III) mutants.

Loss of *cnoe* produces large-scale morphological defects

Reduction or loss of *cnoe* produces several unique phenotypes that are not observed in wild-type embryos. Severe head defects are common, and head involution is often disrupted (Fig. 4A-D, yellow arrows). Head involution begins during germband retraction and continues throughout dorsal closure (VanHook and Letsou, 2007). During head involution, the three preoral and three gnathal tissues that compose the head segments rearrange and migrate internally to form the mouthparts and the anterior end of the digestive system (VanHook and Letsou, 2007). These head tissues remain internal until metamorphosis; at this point, the six tissues come together to form the adult head, which is pushed out of the body cavity to assume its position as the most anterior part of the animal (VanHook and Letsou, 2007).

Defects in head involution are not the only large-scale changes produced when *cnoe* is knocked-down; dorsal closure is also disrupted by the loss of *cnoe*. The lateral epidermis frequently tears away from the amnioserosa, producing gaps in the leading edge (Fig. 4E', red

arrows). Other times, the lateral epidermis does not separate completely from the amnioserosa. At first glance, these instances appear to resemble holes in the leading edge; however, scanning several micrometers below the surface of the lateral epidermis reveals that the leading edge has curled downwards (Fig. 4E', blue arrows). Thus, the leading edge remains continuous, despite spanning more z-planes than typically observed in wild-type embryos.

Loss of *canoe* also produces defects at regions other than the leading edge. Two types of defects are commonly observed in the segmental grooves: segmental groove fusion and abnormally deep segmental grooves. Segmental groove fusion occurs when one segment stretches across the groove and fuses with one or more neighboring segments (Fig. 4F', green arrows). This phenomenon results in the partial or complete disappearance of the groove, depending on where the bridging between neighboring grooves occurs. Segmental grooves in *canoe* mutants are also unusually deep (Fig. 4A-D, purple arrows). The grooves in *canoe* mutants extend closer to the leading edge and deeper into the underlying tissue of the embryo compared to grooves in wild-type flies.

Loss of *canoe* also dramatically impacts epidermal cell shape. Wild-type epidermal cells have a similar columnar shape across the leading edge (Fig 4G', yellow outlines). Additionally, the leading edge typically forms a straight border between the lateral epidermis and amnioserosa (Fig 4G'). These characteristics are strikingly different in *canoe* mutants: epidermal cell shape becomes more variable and more cuboidal, and the leading edge is less continuous (Fig 4H', yellow outlines). These results support the hypothesis that Canoe is an important modulator of AJ/cytoskeletal integrity. In the absence of *canoe*, epithelial cells are unable to maintain proper size and shape when exposed to increased tension and contractile forces.

Loss of *canoe* disrupts wild-type enrichment patterns of adhesion molecules

After examining the large-scale morphological defects produced when *canoe* is knocked-down, we were left with a new question: how does loss of *canoe* affect the enrichment patterns of adhesion molecules?

We began our investigation by examining the localization of E-cadherin, which sits at the core of the AJ. Previous work with *canoe* mutants suggested that Canoe is not essential to maintain adherens junctions or wild-type E-cadherin enrichment (Sawyer et al., 2011; Choi et al., 2016; Cox et al. 1996; Tepass et al., 1996). Therefore, we did not expect *canoe* knockdown to disrupt the localization of E-cadherin. While morphological defects did occur in *canoe* mutants, we observed only slight changes in the enrichment pattern of E-cadherin (Fig. 5A'-B'). In *canoe* knockdown mutants, E-cadherin appears less enriched at the LE-AS border along the leading edge (Fig. 5B', yellow arrows). E-cadherin also appears less enriched at LE-LE cell borders (Fig. 5B', red arrows). These results are consistent with previous conclusions.

Next, we examined whether loss of *canoe* disrupts the localization of actin and the actin-associated molecule, Enabled. The enrichment pattern of actin fibers appears similar in moderate *canoe* mutants and in wild-type embryos during early dorsal closure (Fig. 5C'-D'). During early dorsal closure, actin appears subtly enriched along the leading edge compared to other locations in the embryo (Fig. 5C'-D', yellow arrows). In some instances, *canoe* knockdown mutants show small gaps where actin appears to be absent from the leading edge (Fig. 5D', red arrows). Despite these slight differences, the enrichment pattern of actin fibers remains largely unchanged in *canoe* knockdown mutants. These results suggest that Canoe is not essential to recruit actin fibers to the leading edge; however, the cell shape changes we observed in the lateral epidermis suggest that Canoe does play a role in connecting the actin cytoskeleton to the core AJ

molecules. This organization allows Canoe to translate contractility across the lateral epidermis by regulating AJ/cytoskeletal linkage.

In moderate *canoe* mutants, there is an overall reduction of Enabled at the leading edge (Fig 5E'-F'). Furthermore, the spacing between puncta becomes more variable compared to the regular pattern observed in wild-type embryos (Fig 5E'-F', yellow arrows). These data suggest that Canoe may recruit Enabled to bicellular junctions at the leading edge (Fig. 6). In the absence of Canoe, Enabled does not localize properly to these LE-LE bicellular junctions.

DISCUSSION

Cell adhesion is a fundamental property in animal development, allowing individual epithelial cells to engage in collective migration and enabling the translation of contractile forces across a sheet of epithelial tissue. AJs are the sites where the actomyosin cytoskeleton is linked across the plasma membrane to connect to the cytoskeleton of a neighboring cell. The structure of the AJ enables the junction to perform multiple functions, including the initiation and stabilization of cell-cell adhesion, modulation of the actomyosin cytoskeleton, intracellular signaling, and transcriptional regulation; however, the exact interactions among adhesion molecules located at AJs remain unclear.

Given the broad importance of AJs in animals, we wanted to elucidate the mechanisms by which adhesion molecules regulate AJ/cytoskeletal linkage. Work from many labs has suggested that proteins other than the transmembrane cadherin and cadherin-binding catenins are involved in these interactions. We focused our study on Canoe, one proposed cytoskeletal-junction linker protein.

We began our investigations by examining the enrichment patterns of Canoe and other adhesion molecules during dorsal closure in wild-type *Drosophila* embryos. Dorsal closure serves as an excellent model for collective cell migration and can provide insight into how cell-cell adhesion is modulated at the AJs during embryogenesis. Furthermore, dorsal closure closely resembles epithelial wound healing and neural tube development in higher vertebrates (Agnès and Noselli, 1999; Jacinto et al., 2002). Thus, the results of this study could be generalized to provide insight into similar biological phenomena that are more difficult to manipulate and study.

We examined Canoe, Armadillo, actin, myosin II heavy chain, E-cadherin, and Enabled in wild-type *Drosophila* embryos. We found that Canoe's enrichment pattern aligns closely with the ends of F-actin fibers along the leading edge. These results suggest that Canoe plays a role in modulating the linkage of the actomyosin cytoskeleton to the core catenin-cadherin complex at AJs.

The location of myosin II differs from the location of actin. Whereas actin forms a continuous ring around the dorsal hole, myosin II appears enriched in bright spots located *in between* LE-LE bicellular junctions along the leading edge. These spots of myosin II form an alternating pattern with puncta of Enabled, which appear to localize *at* the bicellular junctions.

These results led us to wonder, what happens to these enrichment patterns when *canoe* levels are reduced in the developing embryo? To examine this question, we generated *canoe* knockdown mutants by utilizing the UAS-Gal4 system in conjunction with RNA interference. Crossing different-strength maternal drivers with different-strength shRNA lines produced *canoe* knockdown mutants with dose-dependent morphogenetic defects.

Results from cuticle preparation data suggest that the strongest *canoe* knockdown mutants can be generated by crossing the strong Mat-Gal4 (II,III) maternal driver with UAS.*cno* RNAi Valium 22 (II). These very strong *canoe* knockdown mutants will be appropriate for examining how near-complete loss of Canoe affects apical constriction and convergent extension during *Drosophila* germband extension. However, because strong *canoe* knockdown produces embryos that are too highly altered by late embryogenesis to obtain useful data, we shifted our focus to more moderate lines of *canoe* knockdown mutants for studies on dorsal closure.

Once we generated *canoe* knockdown mutant lines, we examined how adhesion molecule enrichment patterns are disrupted when zygotic *canoe* is lost or reduced. We focused our

analyses on large-scale morphogenetic defects and on changes in the patterning of Enabled. The *canoe* knockdown mutants displayed severe phenotypic defects that were not observed in wild-type embryos. These defects include the tearing away of the lateral epidermis from the amnioserosa, the curling-under of the leading edge in relation to the apical surface of the lateral epidermis, segmental groove fusion, abnormally deep segmental grooves, and defects in head involution. We found that loss of *canoe* also caused epithelial cells to become more cuboidal in shape compared to the columnar shape observed in wild-type embryos. Furthermore, the number and regularity of puncta of Enabled decreased across the leading edge when *canoe* was knocked-down. These results are consistent with the notion that Canoe acts as an important cytoskeletal-junction linker protein during morphogenesis.

Three interesting phenomena observed during the course of this study will form the bases for future work. First, Armadillo undergoes dramatic relocalization during dorsal closure; Armadillo appears enriched along the LE-AS border during early closure, but relocalizes to LE-LE cell borders as dorsal closure progresses. This change in Armadillo enrichment is an example of cell polarity – the ability to differentially target proteins to distinct plasma membrane domains. Cell polarity is an important cellular property, underlying processes from bacterial motility to neuronal transmission. Recent work has suggested that Canoe plays an important role in establishing epithelial polarity by directing multiple proteins and positioning AJs (Bonello et al., 2018). Future studies will continue to investigate how polarity is initiated and established in epithelial cells using *Drosophila* embryogenesis as a model.

Second, during our examination of actin, data from confocal microscopy studies suggested that actin forms bright spots *at* LE-LE bicellular junctions along the leading edge; however, super-resolution microscopy revealed that actin fibers end just prior to these junctions

(Manning unpublished). This example highlights the conflicts that are sometimes observed between results from confocal microscopy and those obtained from super-resolution microscopy. Future work will employ super-resolution microscopy to re-examine our current conclusions and gain further insight into the localization of AJ-associated molecules.

Finally, initial examination of the protein Polychaetoid suggests that it may also act as a cytoskeletal-junction linker protein. Polychaetoid is homologous to the mammalian junction protein Zonula-Occludens-1 (ZO-1), which is associated with both septate/tight and adherens junctions in humans and mice (Brody 1998). Previous work in the Peifer lab suggests that Canoe and Polychaetoid exhibit similar tissue distribution and appear to colocalize at junctional membrane sites within epithelial cells (Sawyer et al., 2009; Choi et al., 2011). Future work will focus on knocking-down both *polychaetoid* and *canoe* in *Drosophila*. This work will continue Choi et al.'s work with *zo-1* and *afadin* double-mutant MDCK cells (2016). Based on previous experiments, we expect that the dorsal closure phenotypes that we observed with the *canoe* single mutants will be more severe in the *polychaetoid/canoe* double mutants. This study will further our understanding of Canoe's role and its interactions with other junction-linker proteins.

FIGURES AND TABLES

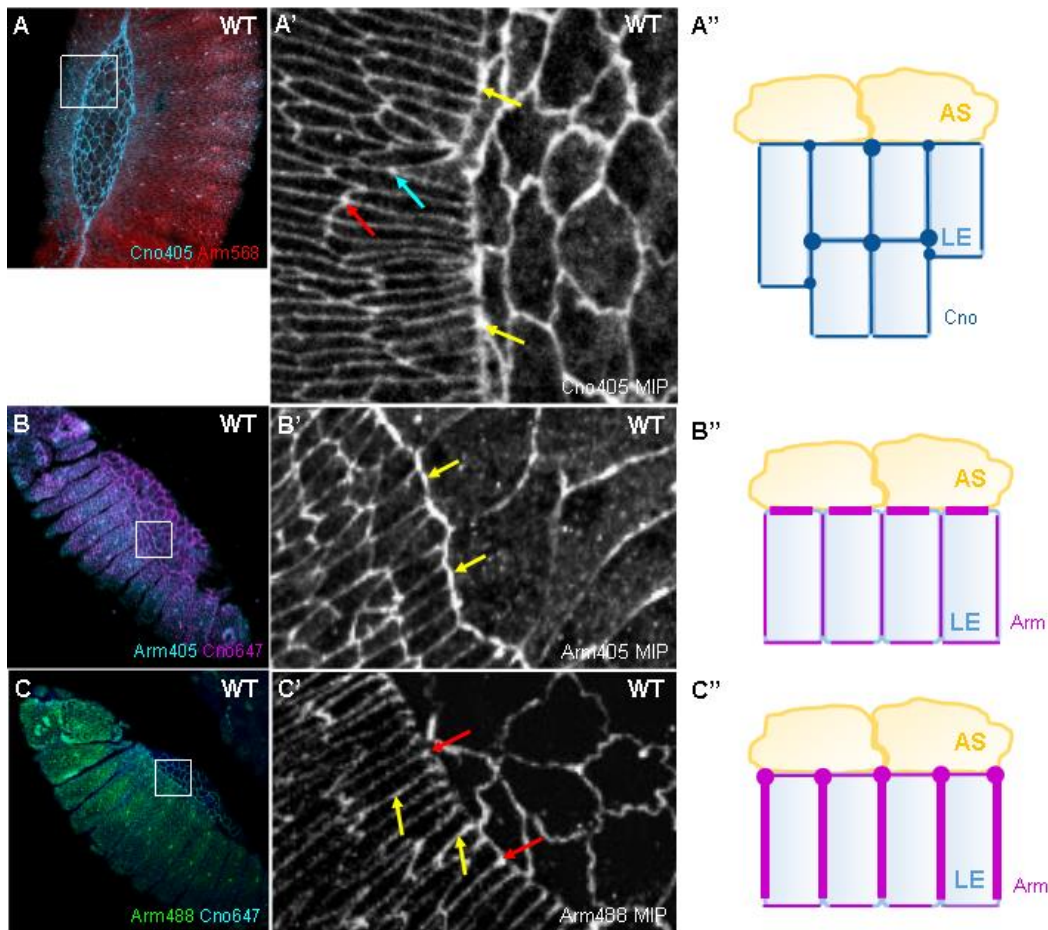


Figure 1. During wild-type dorsal closure, Canoe and Armadillo are enriched at LE cells along the leading edge. (A) Canoe and Armadillo in a wild-type *E-cadherin-GFP* embryo. The white box indicates the region of focus. (A') Canoe appears enriched along the leading edge, particularly at LE-LE bicellular junctions. These areas of enrichment are denoted by yellow arrows. Canoe is also enriched at tri- and multicellular junctions in the lateral epidermis. Tricellular junctions are indicated by blue arrows, and multicellular junctions are indicated by red arrows. (A'') An illustrated representation of the distribution of Canoe in wild-type embryos. (B) Canoe and Armadillo in a wild-type *E-cadherin-GFP* embryo. (B') Compared to Canoe, Armadillo is enriched in the spaces *between* LE-LE bicellular junctions across the leading edge. These areas of enrichment are denoted by yellow arrows. (B'') An illustrated representation of the distribution of Armadillo during early dorsal closure. (C) Canoe and Armadillo in a wild-type *yellow-white* embryo. (C') As dorsal closure progresses, Armadillo relocates to LE-LE cell borders, indicated by yellow arrows. Actin-nucleating centers are indicated by red arrows. (C'') An illustrated representation of the distribution of Armadillo during late dorsal closure.

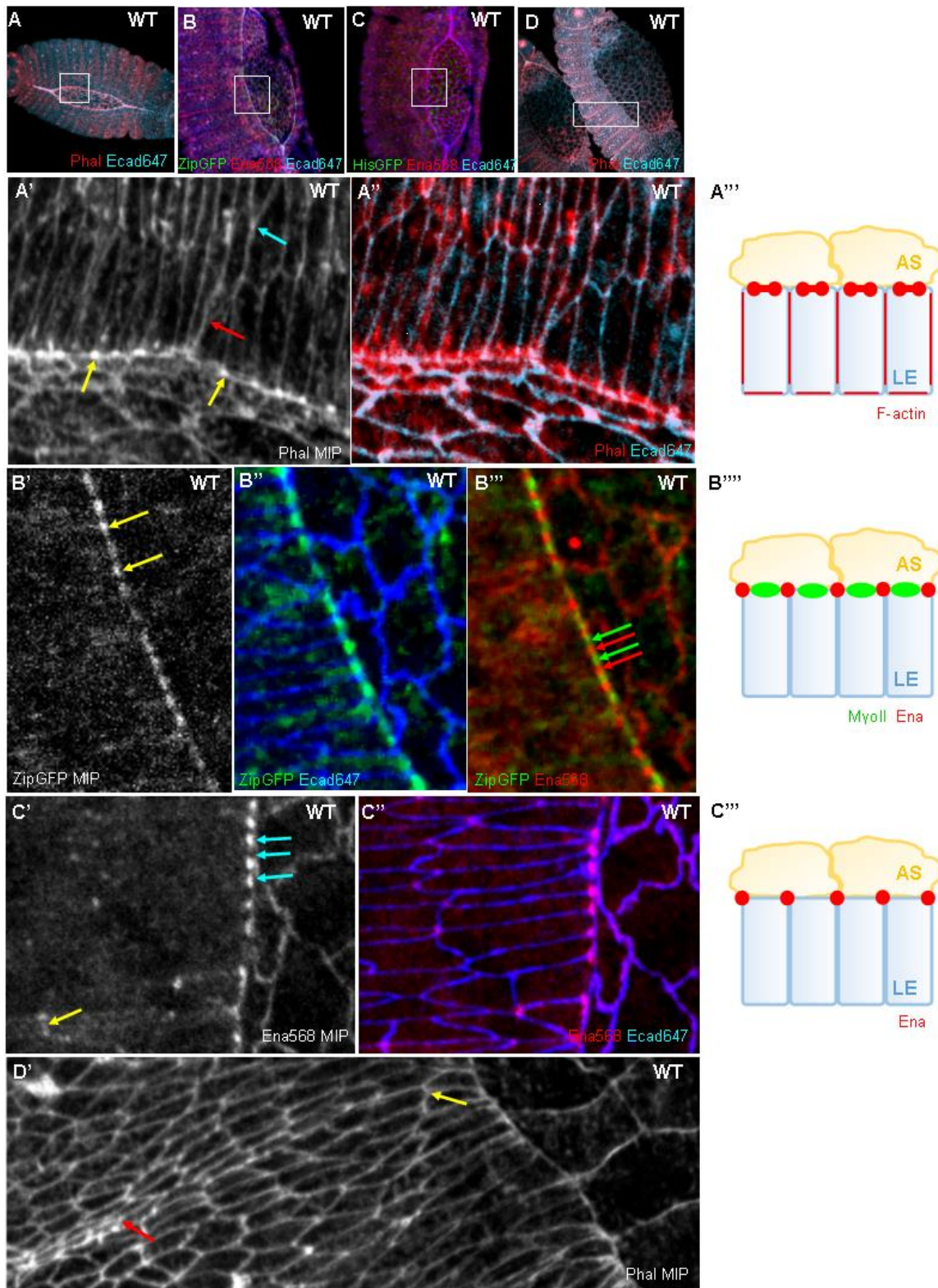


Figure 2. During wild-type dorsal closure, actin appears continuously enriched along the leading edge, while myosin II heavy chain and Enabled form an alternating pattern. (A) E-cadherin and phalloidin in a wild-type *yellow-white* embryo. The white box indicates the region of focus. (A'-A'') Actin is visible around the entire periphery of LE cells, shown by red arrows. Actin appears apically enriched at the leading edge and at multicellular

junctions in the lateral epidermis, indicated by yellow and blue arrows, respectively. This enrichment pattern mirrors Canoe's enrichment pattern, suggesting that Canoe aligns with a subset of cortical F-actin. (A'') An illustrated representation of actin enrichment in wild-type embryos. (B) Myosin II heavy chain, Enabled, and E-cadherin in a wild-type *Zipper-GFP (II)* embryo. (B'-B'') In contrast to actin, myosin II heavy chain appears in bright spots across the leading edge and is less enriched at multicellular junctions in the LE. Myosin II fibers along the leading edge typically appear in the spaces *between* LE-LE bicellular junctions, denoted by yellow arrows. (B'') In contrast, Enabled puncta appear *at* LE-LE junctions along the leading edge. This enrichment gives rise to an alternating sequence of myosin II - Enabled puncta, illustrated by the green and red arrows. (B''') An illustrated representation of the alternating pattern of Enabled and myosin II heavy chain. (C) Histone-GFP, Enabled, and E-cadherin in a wild-type *Histone-GFP* embryo. (C'-C'') Enabled forms a regular pattern of puncta at LE-LE cell junctions along the leading edge, indicated by blue arrows. Enabled also appears subtly enriched around the perimeter of stretch cells at segmental grooves, highlighted by yellow arrows. (C'') An illustrated representation of Enabled in wild-type embryos. (D) E-cadherin and phalloidin in a wild-type *yellow-white* embryo. (D') Actin also appears enriched around the borders of segmental groove cells. Groove cells near the leading edge show moderate actin enrichment, indicated by yellow arrows. Groove cells farther away from the leading edge show increased actin enrichment, highlighted by red arrows.

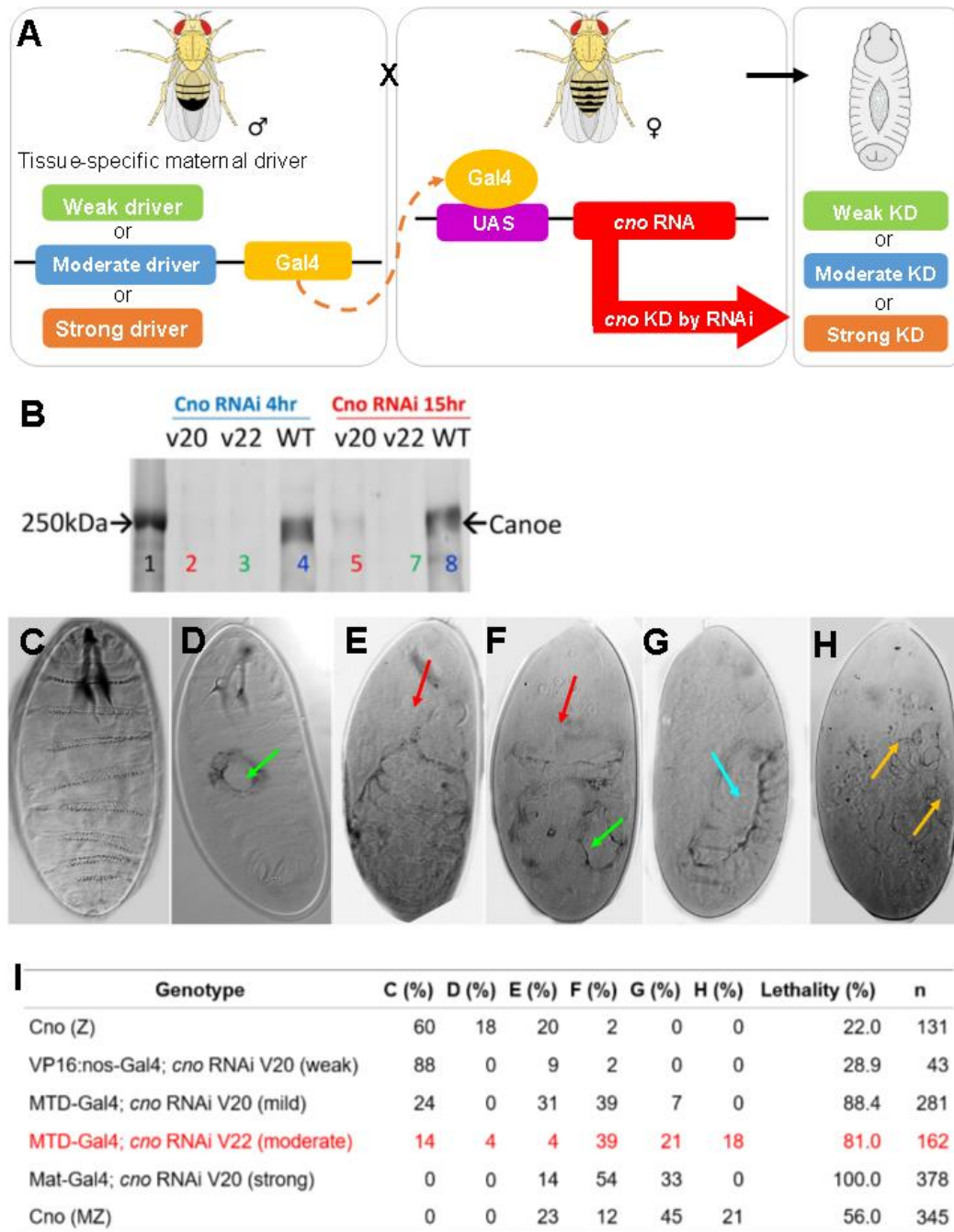


Figure 3. Reducing *canoe* levels results in dose-specific morphological defects. (A) We utilized RNAi and the UAS-Gal4 system to generate lines of *canoe* knockdown mutants. (B) A Western blot of embryo extracts with anti-Canoe antibody indicates that *canoe* knockdown is stronger in UAS.*cno* RNAi Valium 22 (II) mutants (lanes 3, 7) than in UAS.*cno* RNAi Valium 20 (III) mutants (lanes 2, 5). Lanes 4 and 8 represent a wild-type control (Bonello et al., 2018). (C-H) Cuticle preparation data reveals the severity of morphogenetic defects for various-strength *canoe* mutants. Embryo C depicts a wild-type embryo. Embryo D shows mild defects. Embryos E through G depict severe defects. Embryo H depicts the most severe phenotype – only fragmented cuticle pieces remaining. Green arrows represent head or dorsal holes. Red arrows represent head defects. Blue arrows represent the Canoe namesake. Yellow arrows represent cuticle pieces. (I) Cuticle preparation and hatch rate data is tabulated. The black text in the table describes previous work in the Peifer lab (Manning and Sewell, unpublished). The red row in the table highlights new data that was obtained in this study.

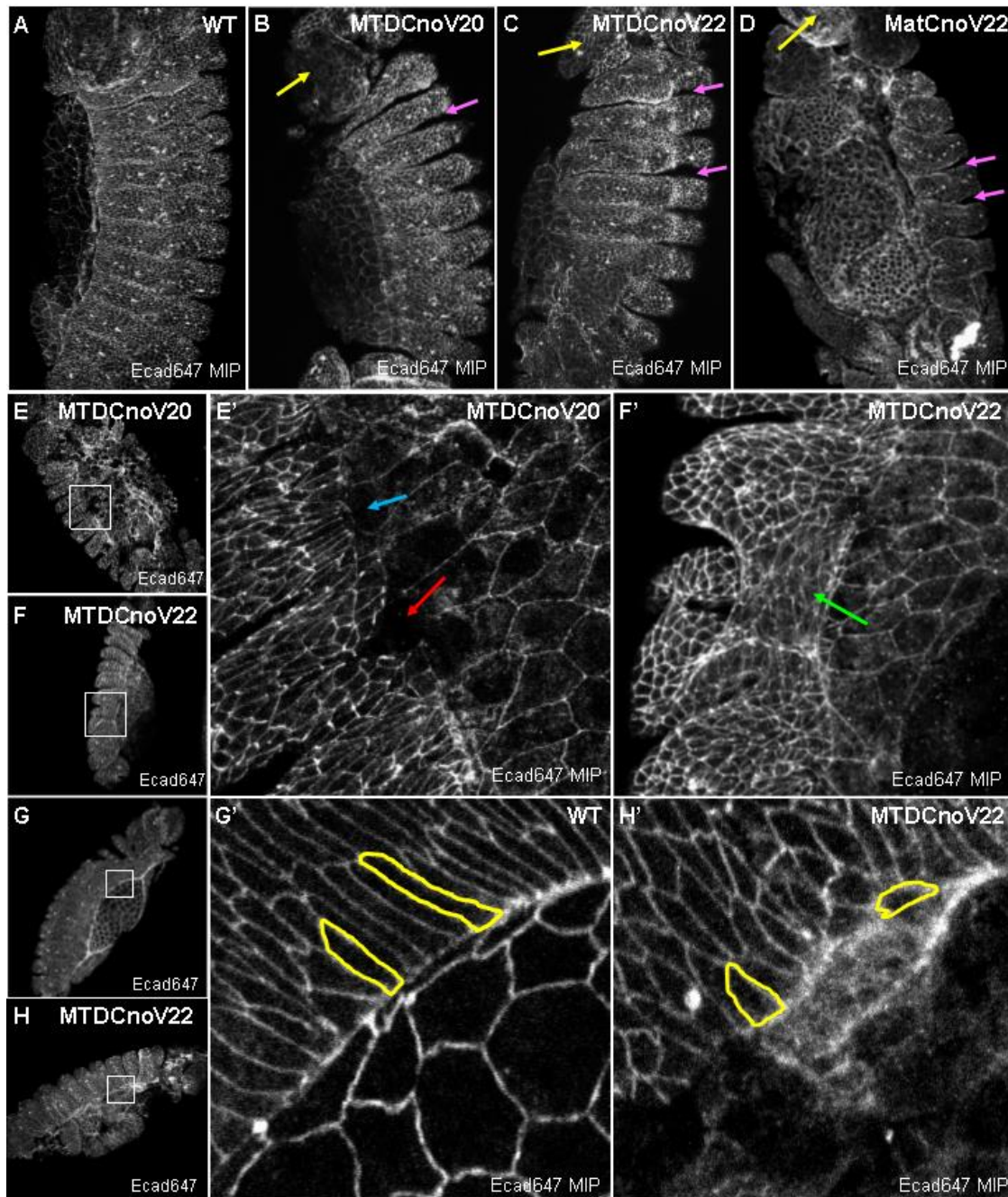


Figure 4. Loss of *canoe* leads to large-scale morphological defects. (A) A wild-type *Histone-GFP* embryo for comparison. (B) In mild *canoe* knockdown mutants, mild defects are observed. Segmental grooves extend closer to the leading edge and penetrate more deeply into the underlying tissue compared to wild-type grooves. These abnormally deep grooves are indicated by purple arrows. Disruption of head involution is highlighted by yellow arrows. (C-D) In stronger *canoe* knockdown mutants, large-scale phenotypic defects appear more severe and are observed more frequently. (E-E') The lateral epidermis is often observed to tear away from the amnioserosa. These torn regions are indicated by red arrows. In some instances, parts of the leading edge curl underneath the surface of the lateral epidermis, indicated by blue arrows. (F-F') Segmental grooves are often observed to fuse in *canoe* mutants. Fused segmental grooves are highlighted by green arrows. (G-G') In wild-type *Histone-GFP* embryos, epidermal cells form regular columnar shapes across the leading edge. (H-H') Epidermal cell shape is dramatically altered in *canoe* knockdown mutants, where epidermal cells appear more cuboidal. The leading edge also appears less straight and more jagged. Yellow outlines highlight examples of LE cells.

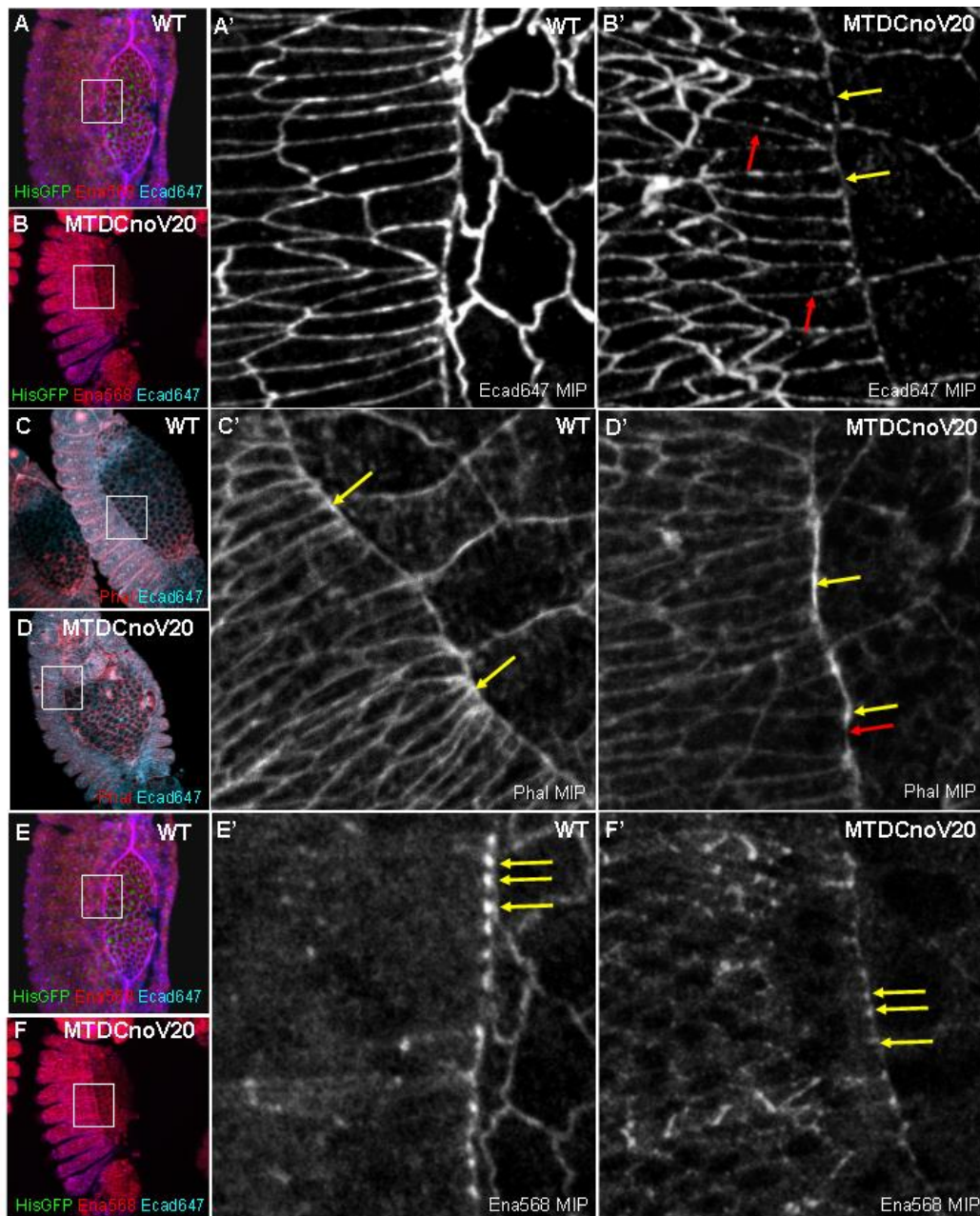


Figure 5. The enrichment pattern of Enabled is dramatically altered in *canoe* knockdown mutants, but E-cadherin and actin do not appear to be significantly disrupted. (A-A') In wild-type *Histone-GFP* embryos, E-cadherin appears only at the periphery of LE and AS cells. (B-B') The enrichment pattern of E-cadherin in *canoe* mutants resembles the pattern observed in wild-type embryos. E-cadherin appears slightly less enriched along the leading edge and at the borders of LE cells adjacent to the leading edge, indicated by yellow and red arrows, respectively. (C-C') In wild-type *yellow-white* embryos, actin fibers appear enriched along the leading edge during early dorsal closure. Actin enrichment is highlighted by yellow arrows. (D-D') A similar pattern is observed in mild *canoe* mutants. Actin enrichment is indicated by yellow arrows, while small areas that appear to lack actin are highlighted by red arrows. These results suggest that Canoe is not essential for localizing E-cadherin or actin filaments to AJs; however, Canoe does play a role in connecting the actomyosin cytoskeleton to the core AJ molecules. (E-E') In wild-type *Histone-GFP* embryos, more Enabled puncta are present, and the spacing between puncta is highly regular. (F-F') In *canoe* mutants, fewer puncta are visible, and spacing between puncta is less regular.

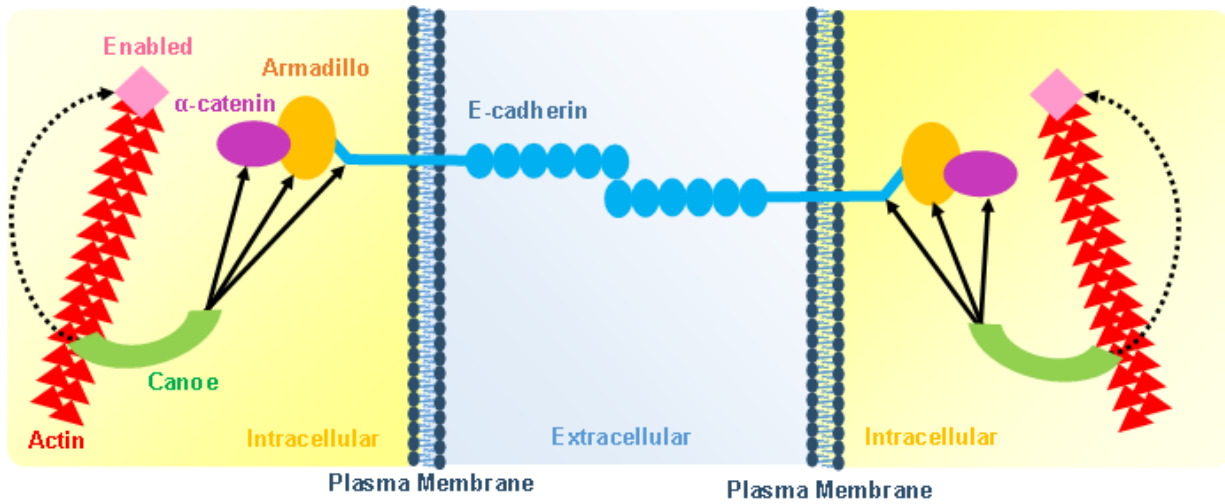


Figure 6. Illustrated representation of the organization of adhesion molecules at AJs. Canoe acts as a cytoskeletal-junction linker protein. Canoe can bind to actin via its F-actin binding domain and can bind to E-cadherin and the catenins via its PDZ and proline-rich domains. Canoe may also recruit the actin-associated molecule Enabled to the AJ. Binding is indicated by solid black arrows while recruitment is indicated by dashed black arrows.

Table 1. Fly stocks, crosses, antibodies, and probes

Stock		Source
MTD-Gal4 (I,II,III) (stock #31777) <i>P{w[+mC]=otu-GAL4::VP16.R}1, w[*];</i> <i>P{w[+mC]=GAL4-nos.NGT}40;</i> <i>P{w[+mC]=GAL4::VP16-nos.UTR}CG6325[MVD1]</i>		Bloomington <i>Drosophila</i> Stock Center (Bloomington, IL, USA)
Mat-Gal4 (II,III) (stock #70630)		Bloomington <i>Drosophila</i> Stock Center
UAS-Gal4 <i>cno</i> RNAi Valium 20 (III) (stock #33367)		Bloomington <i>Drosophila</i> Stock Center
UAS-Gal4 <i>cno</i> RNAi Valium 22 (II) (stock #38194)		Bloomington <i>Drosophila</i> Stock Center

Female Parent	Male Parent	Cross progeny
MTD-Gal4 (I,II,III)	UAS. <i>cno</i> RNAi Valium 20 (III)	MTD-Gal4; MTD-Gal4; MTD-Gal4/ <i>cno</i> RNAi V20
MTD-Gal4 (I,II,III)	UAS. <i>cno</i> RNAi Valium 22 (II)	MTD-Gal4; MTD-Gal4/ <i>cno</i> RNAi V22; MTD-Gal4
Mat-Gal4 (II,III)	UAS. <i>cno</i> RNAi Valium 20 (III)	++; Mat-Gal4; Mat-Gal4/ <i>cno</i> RNAi V20
Mat-Gal4 (II,III)	UAS. <i>cno</i> RNAi Valium 22 (II)	++; Mat-Gal4/ <i>cno</i> RNAi V22; Mat-Gal4

Antibodies and probes	Dilution	Source
Primary antibodies		
Anti-Enabled (mouse)	1:500	Developmental Studies Hybridoma Bank, DSHB
Anti-Armadillo (mouse)	1:200	DSHB
Anti-Canoe (rabbit)	1:1000	J. Sawyer and N. Harris, UNC-CH, NC, USA
Anti-DE-Cadherin (rat)	1:50	DSHB
Secondary antibodies and probes		
Phalloidin FITC	1:500	Sigma Aldrich
Alexa 405, 488, 568, and 647	1:500	Life Technologies

ACKNOWLEDGEMENTS

Dr. Mark Peifer

Dr. Lathiena Manning, Research Mentor and Peifer Lab Member

Dr. Teresa Bonello, Peifer Lab Member

Dr. Andrew Spracklen, Peifer Lab Member

Kia, Perez-Vale, Peifer Lab Member

Dr. John Poulton, Peifer Lab Member

Kristi Schaefer, Peifer Lab Member

Dr. Hui-Chi Yu-Kemp, Peifer Lab Member

Dr. Shiping Zhang, Former Peifer Lab Member

Dr. Wangsun Choi, Former Peifer Lab Member

Tony Perdue, Research Specialist, Microscopy Core

Dr. Steve Rogers, Thesis Reader

Dr. Scott Williams, Thesis Reader

SPIRE Postdoctoral Fellowship

Funding from NIH R01 GM47857, R35 GM18096 and NIGMS K12000678

Funding from the William W. and Ida W. Taylor Faculty-Mentored Research Fellowship, Summer 2017

WORKS CITED

- Agnès, F., and S. Noselli. (1999). Dorsal closure in *Drosophila*: A genetic model for wound healing? *C. R. Acad. Sci. III.* **322**, 5-13.
- Blair, S.S. (2003). Genetic mosaic techniques for studying *Drosophila* development. *Dev.* **130**, 5065-5072.
- Boettner, B., and L. Van Aelst. (2007). The Rap GTPase activator *Drosophila* PDZ-GEF regulates cell shape in epithelial migration and morphogenesis. *Mol. Cell. Biol.* **27**, 7966-7980.
- Boettner, B., P. Harjes, S. Ishimaru, M. Heke, H.Q. Fan, Y. Qin, L. Van Aelst, and U. Gaul. (2003). The AF-6 homolog canoe acts as a Rap1 effector during dorsal closure of the *Drosophila* embryo. *Genetics.* **165**, 159-169.
- Bonello, T.T., K.Z. Perez-Vale, K.D. Sumigray, and M. Peifer. (2018). Rap1 acts via multiple mechanisms to position Canoe and adherens junctions mediate apical-basal polarity establishment. *Development.* **145**:dev157941.
- Brody, T.B. 1998 Feb 15. *Polychaetoid*. Society for Developmental Biology; [accessed 2016 Dec 4]. <http://www.sdbonline.org/sites/fly/cytoskel/polycd1.htm>.
- Brody, T.B. 1998 Feb 18. *Canoe*. Society for Developmental Biology; [accessed 2016 Dec 4]. <http://www.sdbonline.org/sites/fly/dbzhnsky/canoe1.htm>.
- Carmena, A., S. Speicher, and M. Baylies. (2006). The PDZ protein Canoe/AF-6 links Ras-MAPK, Notch and Wingless/Wnt signaling pathways by directly interacting with Ras, Notch and Dishevelled. *PLoS ONE.* **1**, e66.
- Choi, W., B.R. Acharya, G. Peyret, M.A. Fardin, R.M. Mège, B. Ladoux, A.S. Yap, A.S. Fanning, and M. Peifer. (2016). Remodeling the zonula adherens in response to tension and the role of afadin in this response. *J. Cell Biol.* **213**, 243-260.
- Choi, W., K.C. Jung, K.S. Nelson, M.A. Bhat, G.J. Beitel, M. Peifer, and A.S. Fanning. (2011). The single *Drosophila* ZO-1 protein Polychaetoid regulates embryonic morphogenesis in coordination with Canoe/afadin and Enabled. *Mol. Biol. Cell.* **22**, 2010-2030.
- Cox, R.T., C. Kirkpatrick, and M. Peifer. (1996). Armadillo is required for adherens junction assembly, cell polarity, and morphogenesis during *Drosophila* embryogenesis. *J. Cell Biol.* **134**, 133-148.
- Drees, F., S. Pokutta, S. Yamada, W. J. Nelson, and W. I. Weis. (2005). Alpha-catenin is a molecular switch that binds E-cadherin-beta-catenin and regulates actin-filament assembly. *Cell.* **123**, 903-915.
- Franke, J.D., R.A. Montague, and D.P. Kiehart. (2005). Nonmuscle myosin II generates forces that transmit tension and drive contraction in multiple tissues during dorsal closure. *Curr. Biol.* **15**, 2208-2221.
- Gorfinkiel, N. and A.M. Arias. (2007). Requirements for adherens junction components in the interaction between epithelial tissues during dorsal closure in *Drosophila*. *J. Cell Science.* **120**, 3289-2398.
- Gumbiner, B., B. Stevenson, and A. Grimaldi. (1988). The role of the cell adhesion molecule uvomorulin in the formation and maintenance of the epithelial junctional complex. *J. Cell Biol.* **107**, 1575-1587.
- Jacinto, A., S. Woolner, and P. Martin. (2002). Dynamic analysis of dorsal closure in *Drosophila*: From genetics to cell biology. *Dev. Cell.* **3**, 9-19.

- Johnson, M. H., B. Maro, and M. Takeichi. (1986). The role of cell adhesion in the synchronization and orientation of polarization in 8-cell mouse blastomeres. *J. Embryol. Exp. Morphol.* **93**, 239-255.
- Jürgens, G., E. Wieschaus, C. Nüsslein-Volhard, and H. Kluding. (1984). Mutations affecting the pattern of the larval cuticle in *Drosophila melanogaster*. *Roux Arch. Dev. Biol.* **193**, 283-295.
- Kierhart, D.P., C.G. Galbraith, K.A. Edwards, W.L. Rickroll, and R.A. Montague. (2000). Multiple forces contribute to cell sheet morphogenesis for dorsal closure in *Drosophila*. *J. Cell Biol.* **149**, 471-490.
- Mandai, K., Y. Rikitake, Y. Shimono, and Y. Takai. (2013). Afadin/AF-6 and canoe: roles in cell adhesion and beyond. *Prog. Mol. Biol. Transl. Sci.* **116**, 433-454.
- Manning, L.A., M. Sewell, and M. Peifer. (2016). The scaffold protein Canoe and ZO-1 protein Polychaetoid help link cell adhesion and the actomyosin cytoskeleton during tissue formation. N.P.
- Meng, W., and M. Takeichi. (2009). Adherens junction: molecular architecture and regulation. *Cold Spring Harb. Perspect. Biol.* **1**, a002899.
- Müller, H.-A.J., and E. Wieschaus. (1996). Armadillo, bazooka, and stardust are critical for early stages in formation of the zonula adherens and maintenance of the polarized blastoderm epithelium in *Drosophila*. *J. Cell Biol.* **134**, 149-165.
- Pokutta, S., F. Drees, Y. Takai, W.J. Nelson, and W.I. Weis. (2002). Biochemical and structural definition of the I-afadin- and actin-binding sites of alpha-catenin. *J. Biol. Chem.* **277**, 18868-18874.
- Rimm, D.L., E.R. Koslov, P. Kebriaei, C.D. Cianci, and J.S. Morrow. (1995). Alpha 1(E)-catenin is an actin-binding and -bundling protein mediating the attachment of F-actin to the membrane adhesion complex. *Proc. Natl. Acad. Sci. USA.* **92**, 8813-8817.
- Sawyer, J.K., N.J. Harris, K.C. Slep, U. Gaul, and M. Peifer. (2009). The *Drosophila* afadin homologue Canoe regulates linkage of the actin cytoskeleton to adherens junctions during apical constriction. *J. Cell. Biol.* **186**, 57-73.
- Sawyer, J.K., W. Choi, K.C. Jung, L. He, N.J. Harris, and M. Peifer. (2011). A contractile actomyosin network linked to adherens junctions by Canoe/afadin helps drive convergent extension. *Mol. Biol. Cell.* **22**, 2491-2508.
- Scott, J.A., A.M. Shewan, N.R. den Elzen, J.J. Loureiro, F.B. Gertler, and A.S. Yap. (2006). Ena/VASP proteins can regulate distinct modes of actin organization at cadherin-adhesive contacts. *Mol. Biol. Cell.* **17**, 1085-1095.
- Speicher, S., A. Fischer, J. Knoblich, and A. Carmena. (2008). The PDZ protein canoe regulates the asymmetric division of *Drosophila* neuroblasts and muscle progenitors. *Curr. Biol.* **18**, 831-837.
- Staller, M.V., D. Yan, S. Randklev, M.D. Bragdon, Z.B. Wunderlich, R. Tao, L.A. Perkins, A.H. DePace, and N. Perrimon. (2013). Depleting gene activities in early *Drosophila* embryos with the “maternal-Gal4-shRNA” system. *Genetics.* **193**, 51-61.
- Takahashi, K., T. Matsuo, T. Katsube, R. Ueda, and D. Yamamoto. (1998). Direct binding between two PDZ domain proteins Canoe and ZO-1 and their roles in regulation of the jun N-terminal kinase pathway in *Drosophila* morphogenesis. *Mech. Dev.* **78**, 97-111.
- Tepass, U., E. Gruszynski-DeFeo, T.A. Haag, L. Omatyar, T. Torok, and V. Hartenstein. (1996). Shotgun encodes *Drosophila* E-cadherin and is preferentially required during cell rearrangement in the neurectoderm and other morphogenetically active epithelia. *Genes Dev.* **10**, 672-685.

VanHook, A., and A. Letsou. (2007). Head involution in *Drosophila*: Genetic and morphogenetic connections to dorsal closure. *Dev. Dyn.* **237**, 28-38.

Wieschaus, E., and C. Nüsslein-Volhard. (1986). Looking at embryos. *In Drosophila: A Practical Approach*. D.B. Roberts, editor. IRL Press, Oxford, England. 199–228.

Yamada, S., S. Pokutta, F. Drees, W.I. Weis, and W.J. Nelson. (2005). Deconstructing the cadherin-catenin-actin complex. *Cell.* **123**, 889-201.

Young, P.E., A.M. Richman, A.S. Ketchum, and D.P. Kiehart. (1993). Morphogenesis in *Drosophila* requires nonmuscle myosin heavy chain function. *Genes Dev.* **7**, 29-41.